THE JOURNAL OF BIOLOGICAL CHEMISTRY
Vol. 278, No. 11, Issue of March 14, pp. 9835–9842, 2003
Printed in U.S.A.

In Vitro Selection of Adenine-dependent Hairpin Ribozymes*

Received for publication, December 20, 2002, and in revised form, January 6, 2003
Published, JBC Papers in Press, January 7, 2003, DOI 10.1074/jbc.M213058200

Marc Meli, Jacques Vergne, and Marie-Christine Maurel‡

From the Institut Jacques-Monod, Laboratoire de Biochimie de l'Evolution et Adaptabilité Moléculaire, Université Paris VI, Tour 43, 2 place Jussieu, 75251 Paris Cedex 05, France

Adenine-dependent hairpin ribozymes were isolated by *in vitro* selection from a degenerated hairpin ribozyme population. Two new adenine-dependent ribozymes catalyze their own reversible cleavage in the presence of free adenine. Both aptamers have Mg^{2+} requirements for adenine-assisted cleavage similar to the wild-type hairpin ribozyme. Cleavage kinetics studies in the presence of various other small molecules were compared. The data suggest that adenine does not induce RNA self-cleavage in the same manner for both aptamers. In addition, investigations of pH effects on catalytic rates show that both adenine-dependent aptamers are more active in basic conditions, suggesting that they use new acid/base catalytic strategies in which adenine could be involved directly. The discovery of hairpin ribozymes dependent on adenine for their reversible self-cleavage presents considerable biochemical and evolutionary interests because we show that RNA is able to use exogenous reactive molecules to enhance its own catalytic activity. Such a mechanism may have been a means by which the ribozymes of the RNA world enlarged their chemical repertoire.

The RNA world theory assumes that modern life arose from molecular ancestors in which RNA molecules both stored genetic information and catalyzed chemical reactions (1–4). According to this scenario, ribozymes of the RNA world would have been able to self-replicate (5) and to control complex metabolisms with an expanded chemical repertoire (6, 7). Until recently, RNA catalysis was believed to be restricted to phosphate chemistry, but *in vitro* selection experiments and recent discoveries concerning natural ribozymes have demonstrated that the catalytic capacities of RNA are far more promising and exciting than previously anticipated (8–13). However, in comparison with proteins, the chemical spectrum of ribozymes remains limited because of the limited chemical diversity of RNA, which is composed of only four different building blocks.

Yet RNA could increase its range of functionalities by incorporating catalytic building blocks such as imidazole, thiol, and functional amino and carboxylate groups (14, 15). Moreover, primeval nucleotides were not necessarily restricted to standard nucleotides; modified nucleotides may have played a role in catalysis in the RNA world (16, 17).

Another way for RNA to increase its chemical diversity would consist in the binding of exogenous molecules carrying reactive groups and handling them as catalytic cofactors. We recently reported the isolation of new RNA aptamers able to bind adenine in a novel mode of purine recognition (18). Adenine is a likely prebiotic analog of histidine. Its catalytic capabilities are equivalent to histidine because of the presence of a free imidazole moiety (19–21). It was previously shown that when adenine is placed in a favorable microenvironment, its catalytic efficiency is strongly enhanced (22–24). Such favorable microenvironments could result from adenine binding to RNA and thereby providing catalytic sites. In this perspective, it is significant that abasic hairpin and hammerhead ribozymes can be rescued by the addition of exogenous bases that restore activity (25, 26) and that imidazole and cytosine can rescue a cytosine mutation in a self-cleaving hepatitis delta virus ribozyme (27, 28). Also significant is the sequence homology between loop B of the hairpin ribozyme and the XBA aptamer (29), which was selected on the basis of its capacity to bind xanthine and guanine. Hence, the hairpin ribozyme may constitute a good starting point for the search of new ribozymes that require catalytic organic cofactors.

We thus designed a SELEX procedure (systematic evolution of ligands by exponential enrichment) to select inactive hairpin variants capable of recovering activity by the addition of exogenous free adenine. The selection was started from hairpin ribozyme with randomized sequences located in regions previously reported to be required for catalysis. Using this approach, our aim was to maximize the opportunities of selecting new hairpin ribozymes in which adenine restores the activity by its direct involvement in catalysis. Here we report the discovery of two new hairpin ribozymes that require adenine as catalytic cofactor for their reversible self-cleavage.

MATERIALS AND METHODS

Preparation of the Starting RNA Pool—Single-stranded DNA template and primers were synthesized chemically (Genset). The sequence of primer P1 (promoter primer) is 5′-**TAATACGACTCACTATA**GGGTACGCTGAAACAG-3′ (T7 promoter sequence in bold), and that of primer P2 (reverse primer) is 5′-CCTCCGAAACAGGACTGTCAGGGGGTACCAG-3′. The 80-nucleotide-long template consists of the minus strand that allows the synthesis of a hairpin ribozyme randomized in 20 critical positions. Its entire sequence is 5′-CCTCCGAAACAGGACTGTCAGGGGGTACCAGNNNNNNNNNCACAACGTGNNNNNNNNCTGGTTGACNNNNCTGTTTCAGCG-3′. The two primer binding regions are located in the 5′- and 3′-termini. The 20 randomized nucleotides are all located within loops A and B (Fig. 1). The mutations are expected to perturb the geometry of the active site and hence the activity of the ribozyme. The variants to be selected are those that are inactive but whose activity is rescued by free adenine. In contrast to loop B, which is entirely randomized, only the first four unpaired nucleotides of loop A are randomized, because the 3′-unpaired sequence of the loop A is located in the reverse primer binding region that must be kept constant.

A 6-ml PCR (Invitrogen) reaction with 1 μM each primer (P1 and P2) and 0.1 μM template (about 3.4×10^{14} random molecules) amplified by 10 cycles was performed. The random double-stranded DNA pool was then ethanol-precipitated and submitted to *in vitro* transcription (6 ml) using T7 RNA polymerase (Fermentas). The reaction mixture contained 2.5 mM each rNTP, 2 mM spermidine, 10 mM dithiothreitol, 10 mM NaCl, 6 mM $MgCl_2$, 1 μM randomized DNA and 24,000 units of T7 RNA

* This work was supported by grants from CNRS, University Paris VI, and CNES (Centre National d'Etudes Spatiales). The costs of publication of this article were defrayed in part by the payment of page charges. This article must therefore be hereby marked "*advertisement*" in accordance with 18 U.S.C. Section 1734 solely to indicate this fact.

‡ To whom correspondence should be addressed. Fax: 33-1-44-27-59-94; E-mail: maurel@ijm.jussieu.fr.

polymerase. After overnight incubation at 37 °C, the reaction mixture was purified on a 10% denaturing polyacrylamide gel (PAGE), ethanol-precipitated, and resuspended in distilled water, yielding ~10 nmol of randomized RNA.

Selection Procedure—Each selection round consisted in the alternation of negative and positive selection steps followed by reamplification of the selected material. Negative selection steps were performed to eliminate molecules that can self-cleave in the absence of adenine. The RNA was incubated in cleavage buffer (40 mM HEPES, 6 mM $MgCl_2$, pH 7.5) without adenine and purified by 10% denaturing PAGE. Positive selection was performed by incubating uncleaved RNA in cleavage buffer supersaturated with adenine (20–30 mM). The cleaved fragments were purified by denaturing PAGE and amplified by RT-PCR.[1] Additionally, during the last two selection rounds, the 5′-cleaved fragments were selected for adenine-specific religation with the 3′-cleaved fragments; after positive selection for adenine-specific RNA cleavage, purified 5′-cleaved fragments were incubated with a large excess of 3′-cleaved fragments in cleavage buffer. Unligated RNAs were recovered and incubated again with a large excess of 3′-cleaved fragments in the presence of adenine. Religated ribozymes were recovered and amplified.

During each selection round, the randomized RNA pool was dissolved in the cleavage buffer, heated to 65 °C for 3 min, and cooled slowly (3 °C/min) to 23 °C (denaturation and renaturation steps). The solution was then incubated at room temperature, and the cleavage reaction was stopped by adding 1 volume of loading solution (30 mM EDTA, 80% formamide). The RNA concentration was 50 μM in the first generation (G0), and 20–70 μM in the other selection rounds. The reaction times for negative selection were 2–50 h for G0–G9 and 2–4 h for G9–G11, and the negative selections in G0–G8 were repeated. The uncleaved RNAs recovered from the second negative selection were dissolved in cleavage buffer, denatured and renatured, and then incubated with 3 volumes of cleavage buffer supersaturated in adenine. Reaction times for positive selection were 3–20 h for G0–G5 and 10–40 min for G6–G11. After the loading solution had been added to stop the reaction, the cleaved products were purified by denaturing PAGE, ethanol-precipitated (52.5 μg/ml of glycogen was added as carrier), and resuspended in distilled water.

The pooled RNA was reverse transcribed using 20 units/μl Moloney murine leukemia virus reverse transcriptase (MMLV-RT, Invitrogen) with 20 μM reverse primer P2 at 37 °C for 1 h. The cDNA was amplified by PCR with 1 μM each primer (P1 and P2). The thermal cycle program was 94 °C for 30 s, 56 °C for 30 s, and 72 °C for 60 s; the cycle was repeated 16 times. After ethanol precipitation and resuspension in water, the newly selected DNA library served to produce the RNA pool for the next selection round by *in vitro* transcription.

During the last two selection rounds, two additional steps following positive selection were performed to isolate ribozymes able to religate in the presence of adenine. First, adenine-cleaved RNA was dissolved in cleavage buffer in the presence of a 10-fold excess of ligation substrate (LS). LS is a 15-nucleotide-long DNA/RNA mixed oligonucleotide (Genset) in which the sequence corresponds to the 3′-cleaved product (Fig. 1). Its 5′-end is composed of 9 ribonucleotides, and its 3′-terminus is composed of 6 deoxyribonucleotides because 2′-OH are not necessary in this region. Cleaved RNA and LS were heated to 65 °C for 3 min and cooled slowly (3 °C/min) to 8 °C (denaturation and renaturation steps in cleavage buffer prior to ligation). The mixture was incubated at 8 °C for 2 h. The ligation reaction was stopped, and unligated fragments were purified by denaturing PAGE. Finally, the unligated RNAs were again dissolved in cleavage buffer in the presence of a 10-fold excess of LS and then denatured and renatured prior to ligation. Three volumes of a 8 °C cleavage buffer supersaturated with adenine were added, and the solution was incubated at 8 °C for 2 h. The ligated products purified by denaturing PAGE were used for reverse transcription as described above.

After each cleavage or ligation reaction, aliquots (2 μl containing 0.2–1 μg of RNA) were analyzed by denaturing 10% PAGE and ethidium bromide staining. RNA fragments were revealed by UV transillumination and scanned. The light intensities of the fragments were quantified using an NIH Image analyzer. It was thus possible to monitor the evolution of cleavage or ligation efficiencies in the presence or absence of adenine during the selection process.

Cloning—Ribozymes positively selected at G11 were cloned (TOPO TA cloning kit, Invitrogen) after conversion of RNA to double-stranded DNA by RT-PCR. Plasmids were prepared from isolated clones (Plasmix minipreps, Talent), and the cloned DNAs were sequenced. After plasmid purification and *in vitro* transcription of the PCR-amplified inserted fragments, individual RNAs were prepared for further studies.

Cleavage Reactions of Individual RNA Molecules—Double-stranded DNA templates were prepared from individual plasmids by PCR using primers P1 and P2. The RNAs were transcribed from the DNA templates and purified as described above. Individual RNAs (4 μM) were dissolved in cleavage buffer and subjected to the denaturation and renaturation steps. The solutions were then incubated with 3 volumes of cleavage buffer alone (negative controls) or with 3 volumes of adenine containing cleavage buffer (2.7 mM adenine). Aliquots were removed from the mixtures at various times and added to 1 volume of loading solution. After overnight incubation with adenine or 3 days of incubation in cleavage buffer alone, the reactions were analyzed by denaturing PAGE and ethidium bromide staining. The observed rate constant values (k_{obs}) were calculated using the equation $S/(S + L) = a(1 - \exp(-k_{obs}t))$ (30), where S is the concentration of the cleaved product, L the concentration of the precursor, t is time, and a is the percentage of cleaved product *versus* total RNA at equilibrium.

Ligation Reactions of Individual RNA Molecules—Individual RNAs were subjected to overnight adenine-assisted self-cleavage, and the cleaved fragments were purified as described above. Individually cleaved RNAs (4 μM) were dissolved in cleavage buffer with 72 μM LS, denatured, and renatured prior to ligation. The solutions were then incubated with 3 volumes of cleavage buffer either alone (negative controls) or supplemented with 2.7 mM adenine. Reactions were analyzed, and the k_{obs} values were calculated, except that S was taken as the concentration of the ligation product.

Adenine Dependence of Cis-cleavage Reactions—Individual RNAs (4 μM) were dissolved in cleavage buffer. After denaturation and renaturation, 8 aliquots were prepared and incubated with 3 volumes of varying concentrations of adenine in cleavage buffer (0.027 to 20 mM). Aliquots were removed after 30, 60, 90, and 120 min, the cleavage reactions were analyzed, and the k_{obs} were plotted as a function of adenine concentration.

Magnesium Dependence of Cis-cleavage Reactions—Individual RNAs (4 μM) were dissolved in cleavage buffer with $MgCl_2$ concentrations ranging from 0.1 μM to 10 mM. After denaturation and renaturation, the solutions were incubated with 3 volumes of adenine (30 mM) in cleavage buffer with the corresponding $MgCl_2$ concentrations. Aliquots were removed at various times, the cleavage reactions were analyzed, and the k_{obs} values were plotted as a function of $MgCl_2$ concentration.

Cis-cleavage Reactions with Small Molecules—Individual RNAs were dissolved in cleavage buffer and subjected to the denaturation and renaturation steps. Aliquots were incubated with 3 volumes of 3–5 different concentrations of small molecules in cleavage buffer (from 0.1 mM to 150 mM depending on the solubility of the compound). The molecules tested for cis-cleavage were 1-methyladenine, 3-methyladenine, 6-methyladenine, purine, xanthine, hypoxanthine, uracil, and imidazole. Aliquots were removed at various times and analyzed as described above. The k_{obs} values were plotted as a function of small molecules concentrations.

Studies of the pH Dependence of Cis-cleavage Reactions—Individual RNAs were dissolved in cleavage buffers with pH values ranging from 4 to 10 prior to the denaturation and renaturation steps. The buffers used were 40 mM sodium acetate for pH 4 and 5, 40 mM HEPES for pH values from 6 to 8.2, and 40 mM glycine for pH 8.6, 9, and 10. After denaturation and renaturation, the solutions were incubated with 3 volumes of 32 mM adenine dissolved in the cleavage buffers with the respective pH values. Aliquots were removed at various times, and the cleavage reactions were analyzed as described above. The experiment was repeated using 32 mM imidazole instead of adenine and were also performed without cofactor. The k_{obs} values for adenine-assisted cleavage, imidazole-assisted cleavage, and RNA cleavage without cofactor were plotted as a function of pH.

RESULTS

In Vitro Selection—In vitro selection began with a pool of 85-nucleotide-long hairpin ribozymes containing 20 degenerate nucleotides. The randomized positions were all located in loop A (4 randomized nucleotides) and in loop B (16 randomized nucleotides). Degeneracy was introduced in these positions because loops A and B contain the nucleotides required for catalytic activity in the wild-type ribozyme (Fig. 1). Our selection procedure was designed to select inactive ribozymes in which

[1] The abbreviations used are: RT-PRC, reverse transcriptase PCR; LS, ligation substrate; ADHR, adenine-dependent hairpin ribozyme.

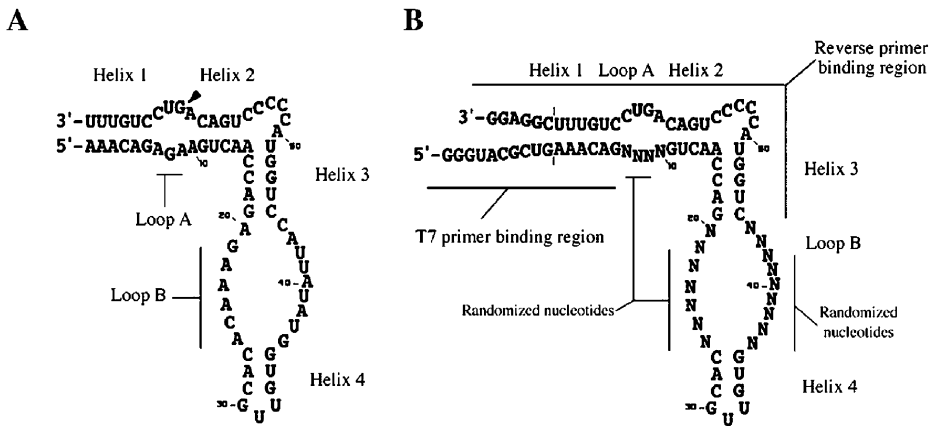

FIG. 1. **Wild-type hairpin ribozyme and randomized starting construct sequences.** *A*, minimal wild-type self-cleaving hairpin ribozyme. The cleavage site is indicated with an *arrowhead*. *B*, randomized construct used for *in vitro* selection. 20 degenerate nucleotides are located within loops A and B at the positions required for catalysis. 3′- and 5′-extensions are added for hybridization with replication primers.

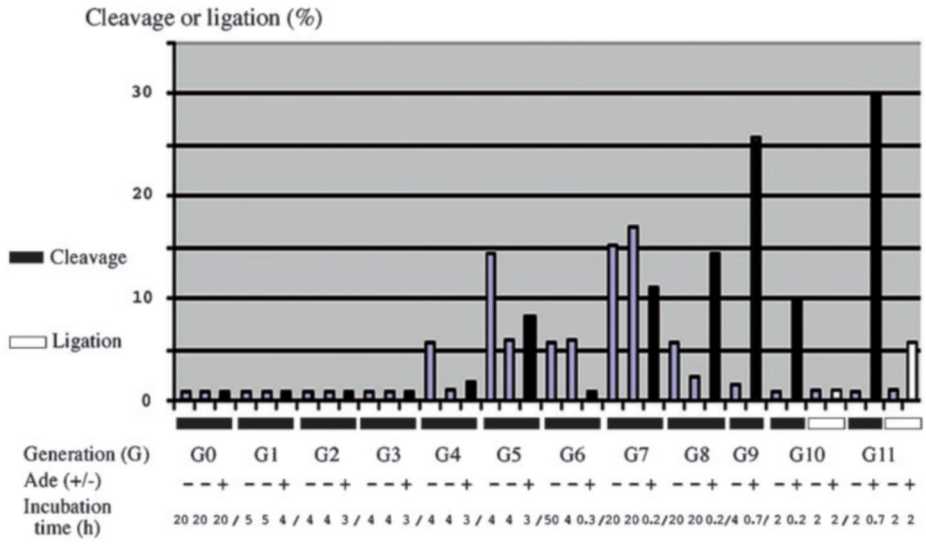

FIG. 2. **Progress of *in vitro* selection.** Self-cleavage or self-ligation percentages during each round of selection. Adenine-assisted cleavage percents are represented by *black bars*, and adenine-assisted ligation percents are represented by *white bars*. RNA self-cleavage and self-ligation percentages without adenine are represented by *gray bars*. The + and − symbols indicate the presence or absence, respectively, of adenine during the incubation of RNA. Incubation times are also indicated at the *bottom* of the figure.

catalytic activity could be rescued by the addition of free exogenous adenine.

The initial RNA population was composed of $\sim 10^{15}$ molecules and expected to express 10^{12} different ribozyme variants. After transcription from the DNA pool, two successive negative selections were carried out by incubating the transcripts in the absence of free adenine. The uncleaved RNAs were isolated by denaturing PAGE and incubated in the presence of free adenine. The 70-nucleotide-long 5′-cleaved products were purified by PAGE. The selected molecules were converted to DNA and amplified by RT-PCR. The alternation of the negative and positive selection steps was repeated for 12 rounds. The progress of *in vitro* selection is shown in Fig. 2.

During the first four selection rounds, the amount of cleaved RNA was too small to be detected after negative or positive selection. RNA cleavage became detectable as of the fifth selection round (G4), but further selection rounds were necessary to eliminate adenine-independent self-cleaving ribozymes from the population. Adenine-cleaved hairpin ribozymes became predominant in the population at G8. Selection for adenine-assisted self-cleavage was continued to G11. From G9 to G11, the second negative selection step was omitted because most of the adenine-independent self-cleaving ribozymes were removed in G8. In addition, during G10 and G11, adenine-cleaved ribozymes also served to select for adenine-assisted religation. After positive selection and purification of the active molecules, the RNA was incubated with a 10-fold molar excess of LS without free adenine. Unligated fragments were purified by PAGE and incubated again with a 10-fold excess of LS in the presence of free adenine (incubation times are shown in Fig. 2). Religated molecules were purified by PAGE and converted to DNA by RT-PCR. During G10, self-cleavage of the negative and positive selections were 1 and 10%, respectively, and the self-ligation product after negative and positive selections for religation were undetectable. During G11, self-cleavage of the negative and positive selections were 1 and 30%, respectively, and self-ligation of the negative and positive selections for religation were 1.5 and 6%, respectively.

Sequence of Clones—The RNA pool selected for adenine-assisted cleavage and religation during G11 was converted to DNA by RT-PCR and cloned. Two different sequences were obtained after sequencing of 14 clones: ADHR1 and ADHR2 (adenine-dependent hairpin ribozyme). The sequences and secondary structures are shown in Fig. 3*A*. The ADHR1 aptamer displays four mutations with respect to the wild-type ribozyme (U20, A36, G38, and C39 instead of A20, G36, A38, and U39 in the wild-type RNA) and the ADHR2 aptamer displays 6 mutations with respect to the wild-type ribozyme (U20, C24, C26, C37, U38 and G39 instead of A20, A24, A26, U37, A38, and U39 in the wild-type RNA). Both aptamers share a common mutation, U20 in place of A20 in the wild-type RNA. As expected, the guanosine located downstream of the cleavage site (G+1), which is not in the initial randomized zone, is conserved. C25 and U42, which were included in the randomized zone, are conserved. These 3 nucleotides are believed to be the major determinants for the stability of the tertiary structure of the wild-type ribozyme by creating H-bond networks that stabilize the ribozyme in its docked conformation (31, 32). It is thus very

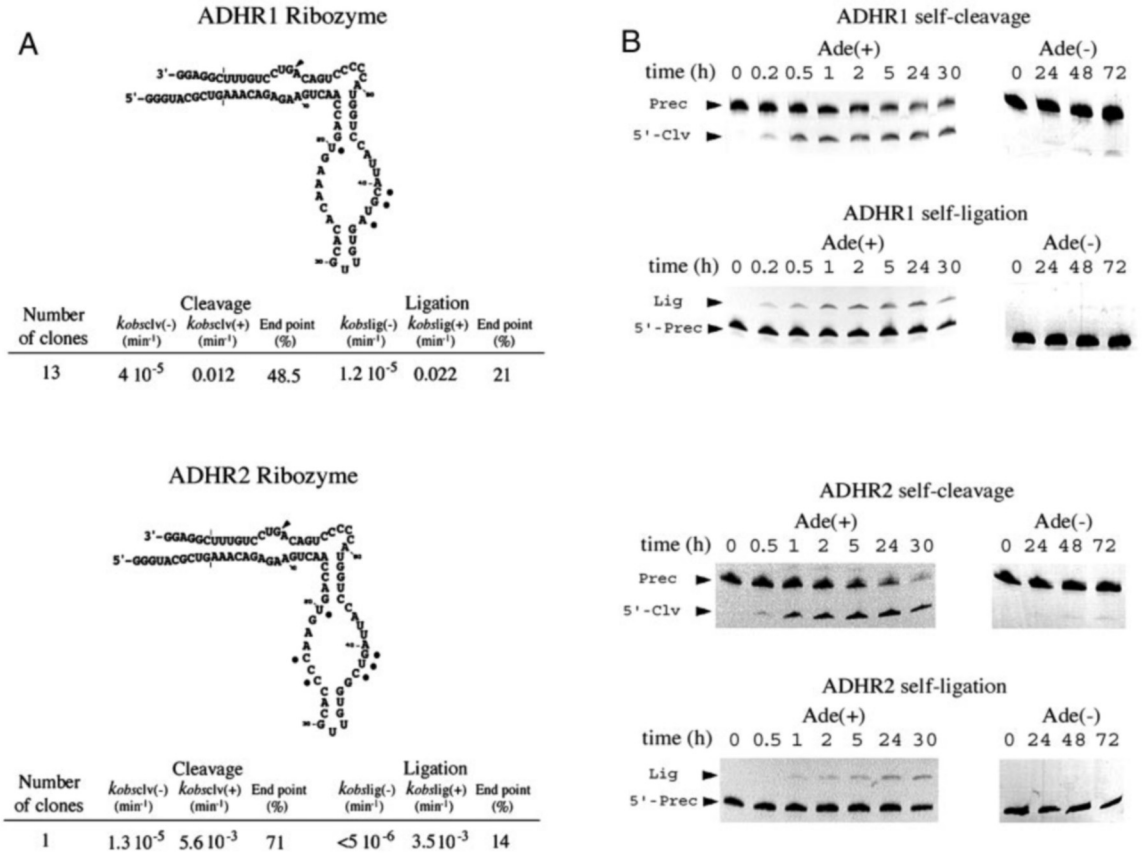

FIG. 3. **Analysis of ADHR1 and ADHR2 self-cleavage and self-ligation activities.** *A*, secondary structures of aptamers. The cleavage site is indicated with an *arrowhead*. Nucleotides that were changed with respect to the wild-type ribozyme are indicated with *gray circles*. Respective k_{obs} and end point values in the presence or absence of adenine are shown under each aptamer secondary structure; + or − symbols indicate that reactions were performed with or without adenine, respectively. *B*, cleavage and ligation kinetics analyzed by 10% denaturing PAGE and ethidium bromide staining. Ade(+) and Ade(−) kinetics were performed with or without adenine, respectively. *Prec*, full-length RNA precursor; *5′-Clv*, 5′ cleaved product; *5′-Prec*, 5′ cleaved product precursor for the ligation reaction; *Lig*, ligation product. *C*, ADHR1 and ADHR2 self-cleavage and self-ligation kinetics plots. *Clv ade*(+) and *Clv ade*(−) indicate that cleavage kinetics were performed with or without adenine, respectively. *Lig ade*(+) and *Lig ade*(−) indicate that ligation kinetics were performed with or without adenine, respectively.

likely that ADHR1 and ADHR2 share the same global docked and active conformation as the wild-type hairpin ribozyme. In contrast, several critical nucleotides of the catalytic site of the wild-type ribozyme were replaced: G36 and A38 were changed to A36 and G38 in ADHR1; A24, A26, and A38 were changed to C24, C26, and U38 in ADHR2. There must be more significant differences in the conformation at the active site of ADHR1 and ADHR2 compared with the wild-type ribozyme because these nucleotides are located in the vicinity of the scissile phosphate (33).

Analysis of Self-cleavage and Self-ligation Activities—Cis-cleavage and cis-ligation activities of both sets of clones were assayed by measuring the k_{obs} in the presence or absence of adenine (Fig. 3). In the experiments carried out without adenine, the rates were too low to reach the end points for which values are needed to calculate the k_{obs}. In effect, after 3 days of incubation of the ribozymes in the absence of adenine, only 2–4% cleavage or ligation was reached. Thus, the k_{obs} values were calculated on the basis of the initial rates of reaction and estimated to be ~10–00-fold higher than the uncatalyzed reaction under the same condition. During cis-cleavage and cis-ligation, each clone has very little activity in the cleavage buffer alone but becomes active with 2.7 mM adenine (values are shown in Fig. 3*A*). The k_{obs} values are in the same order of magnitude for both aptamers. ADHR1 has slightly higher values than ADHR2, and under these experimental conditions the two ribozymes are only 10–30-fold less active than the wild-type ribozyme. These experiments demonstrate that both mutated hairpin ribozyme aptamers are inactive alone but are activated by adenine. Adenine enhances the aptamer cleavage and ligation activities more than 300-fold.

Adenine and $MgCl_2$ Concentration Effects on Cis-cleavage Activity—The k_{obs} values for self-cleavage were measured for both adenine-dependent ribozymes as a function of adenine concentration (Fig. 4*A*). The apparent dissociation constant (K_d) values of ADHR1 and ADHR2 for adenine are 7.6 and 2.6 mM, respectively, and the k_{obs} reached at saturating adenine concentration are 0.04 and 0.011 min^{-1}, respectively. The affinity of ADHR2 for adenine is higher than that of ADHR1, but ADHR1 is more effective at saturating adenine concentration.

The k_{obs} were also measured as a function of $MgCl_2$ concentration (Fig. 4*B*). As expected, millimolar concentrations of Mg^{2+} are required for catalysis. The apparent K_d values of ADHR1 and ADHR2 for Mg^{2+} are 1 and 4 mM, respectively, and k_{obs} reached at saturating $MgCl_2$ concentrations are 0.04 and 0.017 min^{-1}, respectively. ADHR2 needs more Mg^{2+} than ADHR1 to be fully active, and ADHR1 can reach higher activity at saturating Mg^{2+} concentration. In addition, previous studies (34) with comparable wild-type constructs reported 3 mM Mg^{2+} for 50% cleavage k_{obs}, which thus are similar to ADHR1 and ADHR2.

Cis-cleavage Activity with Small Molecules—The k_{obs} values were measured for both adenine-dependent ribozymes in the presence of various concentrations of small molecules (Fig. 5). Both aptamers remain inactive in the presence of 3-methyladenine, xanthine, and uracil. This finding indicates that the N-3

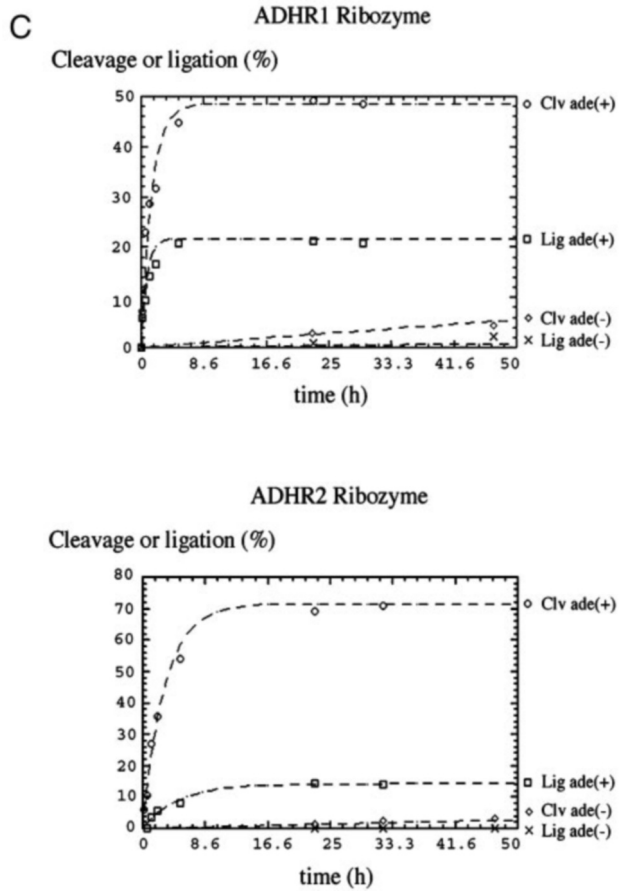

FIG. 3—*continued*

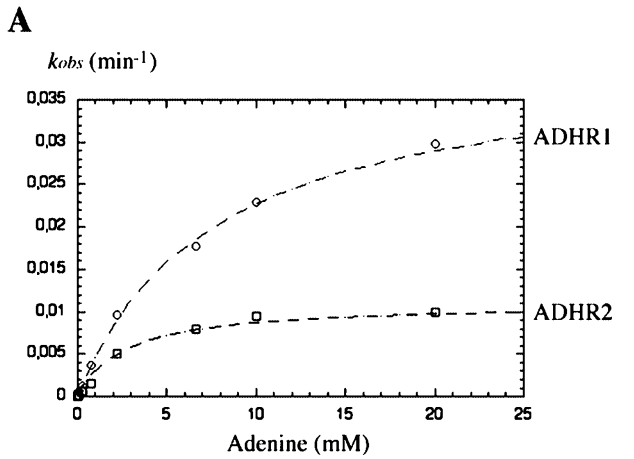

Aptamer	k_{obs}max(adc) (min^{-1})	$K_d$app(ade) (mM)
ADHR1	0.04	7.6
ADHR2	0.011	2.6

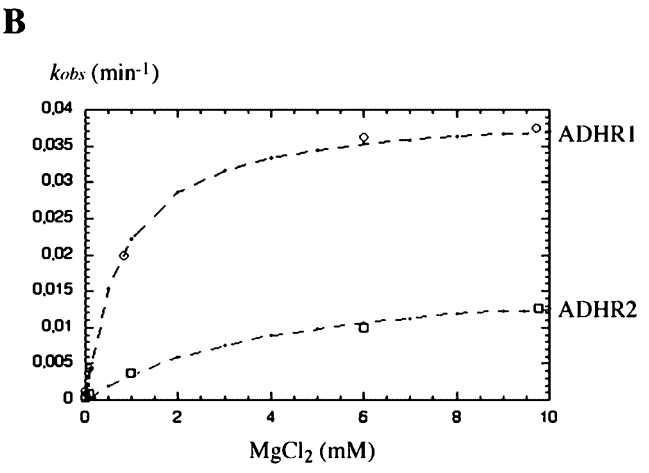

Aptamer	k_{obs}max(Mg) (min^{-1})	$K_d$app(Mg) (mM)
ADHR1	0.04	1
ADHR2	0.017	4

FIG. 4. **Effects of adenine and Mg^{2+} on ADHR1 and ADHR2 catalysis.** *A*, plots of the observed rate constants *versus* adenine concentration. Apparent dissociation constants for adenine ($K_{d\text{app(ade)}}$) and maximal k_{obs} values of each aptamers are shown below the graph. *B*, plots of the observed rate constants *versus* Mg^{2+} concentration. $K_{d\text{app}}$ for Mg^{2+} and maximal k_{obs} values of each aptamer are shown below the graph. The concentration of adenine used in this experiment was 30 mM.

and the C-2 positions of adenine are required for recognition or activation. Low cleavage rates were observed in the presence of hypoxanthine with ADHR1 and ADHR2. Hypoxanthine differs from adenine by substitution of the 6-amino group with a carbonyl group. The K_d values for hypoxanthine are similar to those of adenine. Hypoxanthine thus likely binds both aptamers in the same way as adenine, without inducing the same catalytic effects. Chemical substitutions at position 6 of adenine rather decrease or disrupt catalysis than binding. In effect, ADHR1 retains low activity in the presence of purine and 6-methyladenine. Their K_d values confirm that the 6-amino group of adenine is not involved in ADHR1 recognition. Its absence in purine induces a 40-fold decrease in activity as compared with adenine, but its methylation in 6-methyladenine has no significant effect on activity. Position 6 of adenine is probably involved in hydrogen bond formation required for catalysis. The activation of ADHR1 cleavage induced by imidazole is more striking because, although its affinity is lower compared with adenine, its catalytic efficiency is close to that of adenine (Fig. 5). The imidazole moiety alone is therefore able to induce nearly the same catalytic effect as adenine, even in the absence of its 6-amino group. The imidazole moiety of adenine is thus crucial for catalysis by the ADHR1 ribozyme. In contrast, ADHR2 is capable only of low level self-cleavage in the presence of imidazole. No activity was detected for ADHR2 in the presence of either 6-methyladenine or purine. Compared with the hypoxanthine data, this would mean that the 6-amino group of adenine is able to induce catalysis but not in the same way as ADHR1. Its absence or methylation completely abolishes activity, and its replacement by a carbonyl group yields a 25-fold lower activity with respect to adenine. ADHR2 is active with 1-methyladenine, which has an affinity slightly higher than that of adenine. Substitution at position 1 with a methyl group yields nearly the same catalytic efficiency as adenine. As opposed to ADHR1, which remains inactive with 1-methyladenine, the N-1 atom of adenine is not involved in either ADHR2 recognition or cleavage induction. Taken together, the data related to small molecules indicate that adenine recognition and/or catalysis induction are not achieved in the same manner for ADHR1 and ADHR2.

Effects of pH on Cis-cleavage Activity in the Presence of Adenine and Imidazole—The k_{obs} values at pH ranging from 4 to 10 were measured for both aptamers in the absence or presence

A

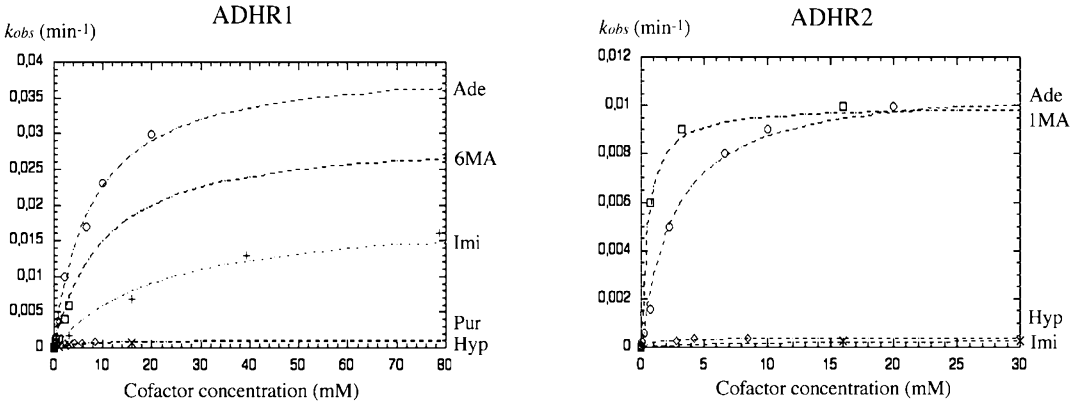

B

		ADHR1		ADHR2	
cofactor	Formula	*kobs*max (min-1)	K*d*app (mM)	*kobs*max (min-1)	K*d*app (mM)
Uracil		N.D.	N.D.	N.D.	N.D.
Xanthine		N.D.	N.D.	N.D.	N.D.
Imidazole		0.019	22	0.00031	15
Hypoxanthine		0.001	3	0.0004	1.5
Purine		0.0016	5.5	N.D.	N.D.
6-methyladenine		0.03	10	N.D.	N.D.
3-methyladenine		N.D.	N.D.	N.D	N.D.
1-methyladenine		N.D.	N.D.	0.01	0.5
Adenine		0.04	7.6	0.011	2.6

FIG. 5. **Effect of adenine analogs on ADHR1 and ADHR2 catalysis.** *A*, plots of the observed rate constants *versus* cofactor concentration. Cofactors used for ADHR1 and ADHR2 self-cleavage are indicated near the corresponding curves. *Ade*, adenine; *1MA*, 1-methyladenine; *6MA*, 6-methyladenine; *Hyp*, hypoxanthine; *Imi*, imidazole; *Pur*, purine. *B*, cofactor affinities and catalytic effects. The maximal k_{obs} and apparent K_d of ADHR1 and ADHR2 for each cofactor are shown. The values are deducted from the curves presented in *A*. *N.D.* indicates that the K_d and k_{obs} values were not detected because activity was too low in the presence of the cofactor.

of cofactor (32 mM adenine or 32 mM imidazole. Plots of k_{obs} as a function of pH for both aptamers are shown in Fig. 6. In the presence of adenine, the k_{obs} values of ADHR1 are very low, between pH 4 and 6. They increase as of pH 6 and reach a plateau between pH 8.6 and 10. The ADHR1 imidazole pH profile is roughly similar to that of the adenine pH profile; the k_{obs} values in the presence of imidazole are higher at low pH but are two times lower at the plateau than in the presence of adenine. Self-cleavage of ADHR1 in buffer alone yields a flat pH profile. The k_{obs} is not measurable at low pH, and self-cleavage becomes detectable at pH 7.5 and increases slightly with pH. At pH 10, k_{obs} values are 55-fold lower than in the presence of adenine and 25-fold lower than in the presence of imidazole). In the presence of adenine, ADHR2 self-cleavage is very low between pH 4 and 5. It increases as of pH 6 to reach a plateau at pH 8.2. The ADHR2 imidazole pH profile is as flat as the ADHR2 pH profile without cofactor. These results suggest that deprotonation events are rate-limiting for adenine-assisted catalysis by both aptamers.

DISCUSSION

The successful selection procedure allowed us to discover new hairpin ribozymes that are strongly dependent on adenine for their reversible self-cleavage reaction. Screening of 14 selected clones yields two different aptamer sequences. ADHR1 is largely prevalent over ADHR2 in the final selected population (13:1). This can be explained by the cleavage and ligation kinetics studies. First, ADHR1 has slightly higher k_{obs} values. Its relative ratio to ADHR2 probably increases after short-time positive selection steps. In addition, two positive selections for religation were performed during the last two selection rounds (Fig. 2). For ADHR1, both the rate and equilibrium constants

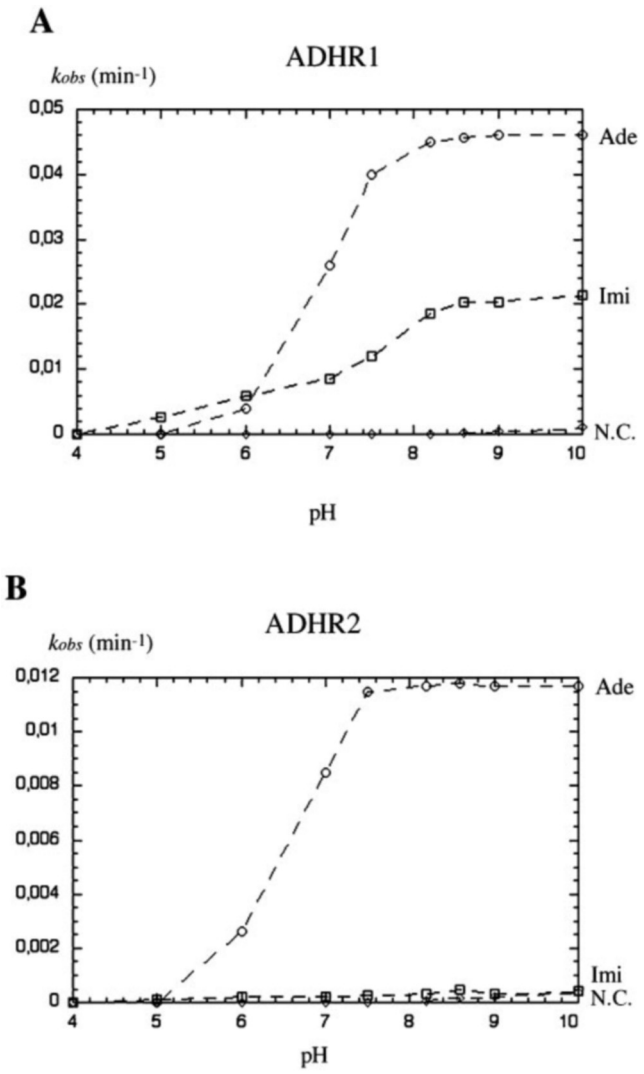

FIG. 6. **Effect of pH on ADHR1 and ADHR2 catalysis.** *A*, plots of the observed rate constants for ADHR1 self-cleavage *versus* pH in the presence of 32 mM adenine or 32 mM imidazole or in the cleavage buffer alone. *B*, plots of the observed rate constants for ADHR2 self-cleavage *versus* pH in the presence of 32 mM adenine or 32 mM imidazole or in the cleavage buffer alone. The identity of the cofactor used is indicated near the corresponding curve. *Ade*, adenine; *Imi*, imidazole; *N.C.*, no cofactor.

for ligation are higher than for ADHR2. Hence, it is easy to understand that ADHR1 predominates over ADHR2 after 12 selection rounds for adenine-assisted cleavage and after two rounds of selection for adenine-assisted religation. This can now be understood in terms of selection conditions. Indeed, ADHR2 requires more Mg^{2+} than ADHR1 does to be fully active. During *in vitro* selection the Mg^{2+} concentration was 6 mM, which is not optimal for ADHR2 catalysis.

The analysis of cis-cleavage and cis-ligation kinetics indicates that the self-cleavage reaction in the presence of adenine is reversible. This confirms that adenine is part of the catalyst and not of the reactants. If adenine were acting as a reactant (for example in direct nucleophilic attack of the scissile phosphate), it would have been trapped either in the 3′- or 5′-side products. In the first case, religation of the 5′-side product with fresh LS (carrying a 5′-OH end) would not have succeeded either in the presence or absence of adenine. In the second case, the 5′-side product would not have religated or would have been able to religate either in the presence or absence of free adenine. ADHR1 and ADHR2 thus catalyze the same kind of reaction as the wild-type hairpin ribozyme. Hydrolysis of the RNA backbone proceeds via the nucleophilic attack of the scissile phosphate by the adjacent 2′-oxygen, and the release products are 2′-3′ cyclic phosphate and 5′-OH termini.

The investigations of the effects of various adenine analogs and the studies of the effects of pH were undertaken to determine the level of implication of adenine in catalytic self-cleavage of ADHR1 and ADHR2. The results of these studies can be explained in several ways. First, it is possible that both aptamers are subjected to a pH-triggered conformational change enhancing catalysis. This remains unlikely, because the pH profile of wild-type ribozyme catalysis is flat between pH 5 and 9 (35). ADHRs 1 and 2 are believed to share a tertiary structure close to that of wild-type, and such a pH-dependent conformational switch observed in both aptamers but absent from the wild-type does not seem very likely. The more probable explanation would be that both aptamers use catalytic strategies in which a deprotonation event (absent or not detectable in the wild-type RNA) is rate-limiting in the chemical cleavage mechanism (acid/base catalysis). Proton transfer would thus be the limiting step in catalysis, and the protons could come from ribozyme chemical groups with shifted pK_a values or from exogenous adenine used as cofactor for cleavage catalysis. Indeed, the use of catalytic Mg^{2+}-complexed hydroxide ions cannot formally be excluded, but this last hypothesis remains very unlikely because the wild-type ribozyme does not use Mg^{2+} in catalysis (36). Indeed, Mg^{2+} dependence of both aptamers is similar to wild-type Mg^{2+} requirements. It is thus probable that ADHR1 and ADHR2 require Mg^{2+} only for folding and not for catalysis *per se*. The involvement of exogenous adenine in direct catalysis is probably different for ADHR1 and ADHR2.

ADHR1 is able to react with a wider variety of adenine analogs than ADHR2. Among these analogs, imidazole (pK_a value, 7) yields comparable catalytic efficiency as adenine. It is thus probable that the imidazole moiety of adenine is involved directly in the catalytic step. The N-9 atom of adenine has a pK_a value of 9.8, which can be shifted toward neutrality as a result of the interaction with ADHR1 RNA. The N-1 atom (pK_a value, 4.1), in which methylation abolishes activity, is also a candidate for acid/base catalysis, but it is not present in imidazole. Models in which N-9- or N-1-deprotonated adenine directly abstract the proton of the 2′-attacking nucleophile oxygen to enhance the catalytic rate (general base mechanism) or chemical mechanisms in which N-9- or N-1-protonated adenine releases its proton to the 5′-oxo leaving groups (general acid mechanism) are thus consistent with our data.

The involvement of adenine in ADHR2 catalysis seems to be different. The imidazole part of adenine seems to be less involved than in ADHR1 catalysis. Methylation of the N-1 atom has no effect on catalysis. Mechanisms involving the adenine N-1 atom with a neutral pK_a available for the abstraction of the 2′ attacking hydroxide proton or for proton release to the 5′-oxo leaving group can thus be excluded for purposes of ADHR2 catalysis. Adenine-assisted ADHR2 self-cleavage seems to be more sensitive than ADHR1 to chemical substitutions at position 6 of adenine. The 6-amino group may thus play a more important role in catalysis by ADHR2 than by ADHR1. We propose two additional chemical explanations. In the first case, ADHR2-bound adenine would simply help to position the RNA reacting groups and would not act directly on catalysis. In the second case, exogenous adenine would act as wild-type ribozyme adenosine 38 by stabilizing the transition state with hydrogen bonds involving its 6-amino group (37). In these two models, the pH profiles of the ADHR2 adenine-assisted self-cleavage would be due to protonation state changes in RNA catalytic groups.

ADHR1 and ADHR2 aptamers do not use the same catalytic

strategies as the wild-type hairpin ribozyme, which is believed to use a transition state stabilization strategy. We have thus selected new hairpin ribozyme variants that are dependent strictly on the presence of exogenous adenine for catalysis. These new adenine-dependent ribozymes act with different catalytic strategies with respect to wild-type ribozyme, probably having different ways of handling exogenous adenine as cofactor for catalysis. These aptamers are of great interest considering the prebiotic RNA world hypothesis. Adenine is itself a prebiotic analog of histidine and could have been used by ribozymes of the RNA world in the same way as histidine is used by present day enzymes. Our work thus supports the view that the use of small exogenous cofactors by ribozymes of the RNA world could have constituted an easy way of expanding its catalytic and metabolic repertoires.

Acknowledgment—We are indebted to Anne-Lise Haenni for valuable suggestions and careful readings of the manuscript.

REFERENCES

1. Woese, C. R. (1965) *Proc. Natl. Acad. Sci. U. S. A.* **54,** 1546–1552
2. Crick, F. H. C. (1968) *J. Mol. Biol.* **38,** 367–379
3. Orgel, L. E. (1968) *J. Mol. Biol.* **38,** 381–393
4. Gilbert, W. (1986) *Nature* **319,** 618
5. Paul, N., and Joyce, G. F. (2002) *Proc. Natl. Acad. Sci. U. S. A.* **99,** 12733–12740
6. Benner, S. A., Ellington, A. D., and Tauer, A. (1989) *Proc. Natl. Acad. Sci. U. S. A.* **86,** 7054–7058
7. Joyce, G. F. (2002) *Nature* **418,** 214–221
8. Doudna, J. A., and Cech, T. R. (2002) *Nature* **418,** 222–228
9. Bartel, D. P., and Unrau, P. J. (1999) *Trends Cell Biol.* **12,** M9–M13
10. Nissen, P., Hansen, J., Ban, N., Moore, P. B., and Steitz, T. A. (2000) *Science* **289,** 920–930
11. Muth, G. W., Ortoleva-Donnelly, L., and Strobel, S. A. (2000) *Science* **289,** 947–950
12. Lilley, D. M. (2001) *Chembiochem* **2,** 31–35
13. Wilson, D. S., and Szostak, J. W. (1999) *Annu. Rev. Biochem.* **68,** 611–647
14. Maurel, M.-C. (1992) *J. Evol. Biol.* **2,** 173–188
15. Cedergren, R., and Grosjean, H. (1987) *BioSystems* **20,** 259–266
16. White, H. B. (1976) *J. Mol. Evol.* **7,** 493–496
17. Trémolières, A. (1980) *Biochimie* (*Paris*) **62,** 493–496
18. Meli, M., Vergne, J., Decout, J. L., and Maurel, M.-C. (2002) *J. Biol. Chem.* **277,** 2104–2111
19. Maurel, M.-C., and Ninio, J. (1987) *Biochimie* (*Paris*) **69,** 551–553
20. Maurel, M.-C., and Convert, O. (1990) *Orig. Life Evol. Biosph.* **20,** 43–48
21. Maurel, M.-C., and Décout, J. L. (1992) *J. Mol. Evol.* **35,** 190–195
22. Décout, J. L., Vergne, J., and Maurel, M.-C. (1995) *Macromol. Chem. Phys.* **196,** 2615–2624
23. Ricard, J., Vergne, J., Decout, J. L., and Maurel, M.-C. (1996) *J. Mol. Evol.* **43,** 315–325
24. Maurel, M.-C., and Décout, J. L. (1999) *Tetrahedron* **55,** 3141–3182
25. Lebruska, L. L., Kuzmine, I. I., and Fedor, M. J. (2002) *Chem. Biol.* **9,** 465–473
26. Peracchi, A., Beigelman, L., Usman, N., and Herschlag, D. (1996) *Proc. Natl. Acad. Sci. U. S. A.* **93,** 11522–11527
27. Perrotta, A., Shih, I.-H., and Been, M. D. (1999) *Science* **286,** 123–126
28. Shih, I.-H., and Been, M. D. (2002) *Proc. Natl. Acad. Sci. U. S. A.* **98,** 1489–1494
29. Kiga, D., Futamura, Y., Sakamoto, K., and Yokoyama, S. (1998) *Nucleic Acids Res.* **26,** 1755–1760
30. Komatsu, Y., Nobuoka, K., Karino-Abe, N., Matsuda, A., and Ohtsuka, E. (2002) *Biochemistry* **41,** 9090–9098
31. Wilson, T. J., Zhao, Z.-Y., Maxwell, K., Kontogiannis, L., and Lilley, D. M. J. (2001) *Biochemistry* **40,** 2291–2302
32. Klostermeier, D., and Millar, D. P. (2002) *Biochemistry* **41,** 14095–14102
33. Rupert, P. B., and Ferré-D'Amaré, A. R. (2001) *Nature* **410,** 780–786
34. Chowrira, B. M., Berzal-Herranz, A., and Burke, J. M. (1993) *Biochemistry* **32,** 1088–1095
35. Nesbitt, S., Hegg, L. A., and Fedor, M. J. (1997) *Chem. Biol.* **8,** 619–630
36. Young, K. J., Gill, F., and Grasby, J. A. (1997) *Nucleic Acids Res.* **25,** 3760–3766
37. Ruppert, P. B., Massey, A. P., Sigurdsson, S. T., and Ferré-d'Amaré, A. R. (2002) *Science* **298,** 1421–1424